Published in final edited form as:
Heart Rhythm. 2013 April ; 10(4): 575–582. doi:10.1016/j.hrthm.2012.12.017.

Pro- and antiarrhythmic effects of ATP-sensitive potassium current activation on reentry during early afterdepolarization-mediated arrhythmias

Marvin G. Chang, PhD[*], **Enno de Lange, PhD**[*], **Guillaume Calmettes, PhD**[*], **Alan Garfinkel, PhD**[*,†], **Zhilin Qu, PhD**[*], and **James N. Weiss, MD**[*,‡]

[*]Department of Medicine (Cardiology), David Geffen School of Medicine at University of California, Los Angeles, California

[†]Department of Integrative Biology and Physiology, David Geffen School of Medicine at University of California, Los Angeles, California

[‡]Department of Physiology, David Geffen School of Medicine at University of California, Los Angeles, California

Abstract

BACKGROUND—Under conditions promoting early afterdepolarizations (EADs), ventricular tissue can become bi-excitable, that is, capable of wave propagation mediated by either the Na current (I_{Na}) or the L-type calcium current ($I_{Ca,L}$), raising the possibility that $I_{Ca,L}$-mediated reentry may contribute to polymorphic ventricular tachycardia (PVT) and torsades de pointes. ATP-sensitive K current (I_{KATP}) activation suppresses EADs, but the effects on $I_{Ca,L}$-mediated reentry are unknown.

OBJECTIVE—To investigate the effects of I_{KATP} activation on $I_{Ca,L}$-mediated reentry.

METHODS—We performed optical voltage mapping in cultured neonatal rat ventricular myocyte monolayers exposed to BayK8644 and isoproterenol. The effects of pharmacologically activating I_{KATP} with pinacidil were analyzed.

RESULTS—In 13 monolayers with anatomic $I_{Ca,L}$-mediated reentry around a central obstacle, pinacidil (50 μM) converted $I_{Ca,L}$-mediated reentry to I_{Na}-mediated reentry. In 33 monolayers with functional $I_{Ca,L}$-mediated reentry (spiral waves), pinacidil terminated reentry in 17, converted reentry into more complex I_{Na}-mediated reentry resembling fibrillation in 12, and had no effect in 4. In simulated 2-dimensional bi-excitable tissue in which $I_{Ca,L}$- and I_{Na}-mediated wave fronts coexisted, slow I_{KATP} activation (over minutes) reliably terminated rotors but rapid I_{KATP} activation (over seconds) often converted $I_{Ca,L}$-mediated reentry to I_{Na}-mediated reentry resembling fibrillation.

Address reprint requests and correspondence: Dr James N. Weiss, Division of Cardiology, David Geffen School of Medicine at University of California Los Angeles, 3641 MRL Bldg, 650 Charles E. Young Drive South, Los Angeles, CA 90095. jweiss@mednet.ucla.edu.
The first 2 authors contributed equally to this work.
Current address of Dr de Lange: Department of Knowledge Engineering, Maastricht University, Maastricht, The Netherlands.

CONCLUSIONS—I_{KATP} activation can have proarrhythmic effects on EAD-mediated arrhythmias if $I_{Ca,L}$-mediated reentry is present.

Keywords

Early afterdepolarizations; Reentry; Bi-excitability; Torsades de pointes; ATP-sensitive K channels; Pinacidil

Introduction

In normal ventricular and atrial tissue, wave-front propagation is driven by activation of the Na current (I_{Na}). Recently, we showed that under conditions promoting early afterdepolarizations (EADs), ventricular tissue can become bi-excitable, that is, capable of wave propagation mediated by either the I_{Na} or the L-type calcium current ($I_{Ca,L}$), separately or simultaneously, in the same tissue.[1] This raises the possibility that in addition to focal activations, $I_{Ca,L}$-mediated reentry may contribute to EAD-mediated arrhythmias such as polymorphic ventricular tachycardia (PVT) and torsades de pointes (TdP). Consistent with this possibility, $I_{Ca,L}$-mediated rotors exhibit a much longer cycle length than I_{Na}-mediated rotors, more compatible with the typical rates of PVT and TdP, and their core meandering reproduces characteristic electrocardiographic features of PVT and TdP.[1]

Many experimental and clinical studies[2–9] have shown that pharmacological activation of sarcolemmal ATP-sensitive K (K_{ATP}) channels shortens action potential (AP) duration and abolishes EADs, preventing EAD-mediated triggered activity and suppressing PVT and TdP.[2–9] Since hypotension is a common consequence of PVT and TdP, the resulting ischemia-related K_{ATP} channel activation may be a factor contributing to spontaneous termination of PVT and TdP and restoration of sinus rhythm by abolishing EAD-mediated focal excitations. Occasionally, however, TdP or PVT degenerate into ventricular fibrillation (VF), causing sudden cardiac death.[10–12] Why most episodes of TdP or PVT terminate spontaneously, but some degenerate into VF, is poorly understood. To explore these issues, we investigated the effects of K_{ATP} channel activation on $I_{Ca,L}$-mediated reentry, given its potential relevance to PVT and TdP. By using optical voltage mapping in neonatal rat ventricular myocyte (NRVM) monolayers, combined with computer simulations, we find that the activation of K_{ATP} channels often terminates $I_{Ca,L}$-mediated reentry but also has a significant probability of converting $I_{Ca,L}$-mediated reentry into I_{Na}-mediated reentry, which can then degenerate into multiwavelet or mother rotor VF, especially if ATP-sensitive K current (I_{KATP}) activation occurs rapidly.

Methods

All protocols used conform to the standard set forth by the National Institutes of Health in the *Guide for the Care and Use of Animals* (NIH Publication No 85-23, revised 1996).

Monolayer preparation

We created monolayers of NRVMs by plating 1×10^6 cells on 21-mm fibronectin-coated plastic coverslips, as previously described.[13] Briefly, the hearts harvested from 2- to 3-day-

old neonatal Sprague-Dawley rats were digested with collagenase (0.02; Worthington Biochemical Corp, Lakewood, NJ) and pancreatin (0.06; Sigma-Aldrich, St Louis, MO). Myocytes were isolated with the use of a Percoll (Pharmacia Biotech AB, Uppsala, Sweden) gradient and plated at a density of 10^6 cells/mm^3 per coverslip.

Optical mapping

Arrhythmias were imaged by optical mapping performed after 11–14 days in culture. Coverslips were visually inspected under a microscope, and monolayers with obvious gaps in confluence were discarded. Acceptable coverslips were then stained with the voltage-sensitive dye di-4-ANEPPS (5 μmol/L for 5 minutes), after which they were continuously superfused with warm (36 °C) oxygenated (normal) Tyrode's solution containing 135 mM NaCl, 5.4 mM KCl, 1.8 mM $CaCl_2$, 1 mM $MgCl_2$, 0.33 mM NaH_2PO_4, 5 mM HEPES, and 5 mM glucose.

APs were recorded by using a charge-coupled device-based optical imaging system (Photometrics Cascade 128+;128 × 128 pixels). Voltage signals were acquired continuously over 10–180 seconds at 0.6–5 ms/frame. Signals were digitized with 16 bits of precision and processed offline, as described previously.[14] Data were stored, displayed, and analyzed by using custom software written in Visual C++ (Microsoft) and MATLAB (MathWorks).

Experimental protocols

Reentrant arrhythmias were initiated by either rapid pacing or incubating monolayers in the presence of the L-type Ca channel agonist BayK8644 (BayK, 2.5 μM) and the beta-adrenergic receptor agonist isoproterenol (Iso; 1 μM) for > 2 hours. The dependence of wave propagation on I_{Na} vs $I_{Ca,L}$ was tested in the subset of monolayers exhibiting reentry (n = 10) by using the Na channel blocker tetrodotoxin (TTX; 50 μM) or the Ca channel blocker nitrendipine (5 μM). K_{ATP} channels were activated by adding pinacidil (100 μM) to the superfusate.

Data analysis

The baseline drift due to photobleaching of potentiometric dyes was reduced by subtracting a third-order polynomial best fit curve of the optical signals. To reduce noise in the optical signals, a 7-point median filter was applied to the detrended data. Movies of electrical propagation were generated from signals that were low-pass filtered between 0 and 100 Hz. The activation time was defined as the instant of maximum positive slope. For each data set, the mean and accompanying 95 confidence intervals are reported. The conventional percentile bootstrap-resampling approach with 10,000 replications was used for estimating 95 confidence interval.[15] A P value of <.05 was considered statistically significant. Conduction velocity was estimated as described previously.[1,14]

Computer simulations

Computer simulations used the ventricular AP model by Mahajan et al,[16] modified to produce EADs and bi-excitability[1]. I_{KATP}, based on the formulation by Ferrero et al,[17] was added to the myocyte model with a density of 3.8 channels/μm^2. To simulate the effects of pinacidil, we increased the fraction of open K_{ATP} channels (f_{ATP}) from 0 to 0.0025 (over

time periods of 50 ms, 10 seconds, or 5 minutes). All simulations were performed in a monodomain 2-dimensional (2D) tissue of 300 × 300 cells (4.5 cm × 4.5 cm), as described previously.[1] A linear gradient in the maximum conductance of I_{Ks} from 0.512 to 2.048 mS/cm^2 was imposed from center to periphery in the tissue to facilitate the joint appearance of both I_{Na}- and $I_{Ca,L}$-mediated wave fronts as described previously to mimic the electrocardiographic appearance of TdP.[1] Simulations were performed on NVIDA Tesla C2050 General Purpose Graphics Processing Units.

Results

Effects of pinacidil on $I_{Ca,L}$-mediated reentry in NRVM monolayers

To generate $I_{Ca,L}$-mediated wave propagation and reentry, we used our previously characterized model of bi-excitability by superfusing NRVM monolayers with BayK + Iso.[1,18] When exposed to BayK + Iso, monolayers developed bursts of EAD-mediated focal activity, typically arising from multiple sites, resulting in a complex mixture of focal activity and reentry, as illustrated in Figure 1. The accompanying optical voltage trace recorded from a representative site in the monolayer during the initiation of a burst of focal activity illustrates the incomplete repolarization between beats, which is consistent with EAD-mediated triggered activity as described previously under these conditions.[1]

Since reentry during BayK + Iso-induced arrhythmias in NRVM monolayers tended to be complex and intermittent due to meandering and frequent interruption by focal activations, we prefabricated monolayers with a hole in the center, which facilitated stable $I_{Ca,L}$-mediated reentry by anchoring reentry and also preventing spontaneous termination due to the core meandering and colliding with a tissue border. In these monolayers, incubation with BayK + Iso frequently resulted in sustained arrhythmias owing to either sustained reentry around the central obstacle (Figures 2 and 3) or more complex patterns in which rotors due to functional reentry were present (Figures 4 and 5). Both anchored and functional reentry in the presence of BayK + Iso were dependent on $I_{Ca,L}$-mediated wave propagation since reentry was consistently abolished by the L-type Ca channel blocker nitrendipine (n = 10) but not by the Na channel blocker TTX (n = 13) as in the examples of reentry around the central obstacle in Figures 2 and 3. Although TTX did not abolish reentry, it made conduction velocity more uniform in some monolayers by slowing rapid propagation in some regions (Figure 3). This indicates that although reentry was dependent on $I_{Ca,L}$-mediated wave propagation, I_{Na} contributed to more rapid propagation in some regions of the monolayer. Thus, BayK + Iso-treated monolayers contained a mixture of $I_{Ca,L}$-and I_{Na}-mediated wave propagation, even though reentry was dependent on $I_{Ca,L}$ rather than I_{Na}.

We then examined the effects of K_{ATP} channel activation with 5 μM pinacidil in monolayers with sustained anatomic or functional $I_{Ca,L}$-mediated reentry for > 10 minutes. In 13 monolayers with sustained anatomic reentry around the central obstacle, as in Figures 2 and 3, pinacidil did not terminate reentry but changed its pharmacological profile. Although reentry was consistently terminated by nitrendipine (Figure 2B) but not by TTX before pinacidil (Figures 2A and 3), the converse was true after pinacidil; that is, reentry was terminated by TTX in all monolayers tested, whereas nitrendipine terminated reentry in only 2 of 10 monolayers tested (20) (Figure 6). This result indicates that pinacidil converted

$I_{Ca,L}$-mediated reentry to I_{Na}-mediated reentry. Consistent with this interpretation, conduction velocity after pinacidil increased by an average of 89 ± 82% (95% confidence interval 46–141) (Figure 7A). This is illustrated by the increased spacing of the isochrone lines after pinacidil in the example shown in Figure 7B.

In contrast, among 33 monolayers with more complex arrhythmia patterns involving functional $I_{Ca,L}$-mediated rotors as in Figures 4 and 5, the administration of pinacidil spontaneously terminated the arrhythmia in 17 (52%) (Figure 4). In the remaining 16 monolayers, complex reentry persisted after pinacidil, but with a significantly shorter average cycle length (Figure 5). In 4 monolayers (12%), the complexity of reentry was not significantly changed (Figure 5 A), but in 12 (36%), the complexity increased with the appearance of many additional and more frequent wave fronts (Figure 5B).

Computer simulations in 2D tissue

To ions by using the Mahajan et al[16] ventricular AP model, with parameters modified to produce EADs with bi-excitable wave propagation in tissue, as described previously. In homogeneous 2D tissue, either I_{Na}- or $I_{Ca,L}$-mediated reentry could be induced, depending on the stimulation protocol used to initiate reentry, indicative of bi-excitability. To study the effects of I_{KATP} activation on functional reentry driven by an $I_{Ca,L}$-mediated rotor in which I_{Na}-mediated wave fronts were also intermittently present (as previously documented in bi-excitable monolayers[1]), we created a heterogeneous 2D tissue with a linearly increasing gradient in I_{Ks} from center to periphery, such that the center of the tissue had a longer AP duration than did the periphery. When an $I_{Ca,L}$-mediated rotor was induced, the rotor meandered throughout the central region, with the arm of the rotor in the outer tissue containing a mixture of $I_{Ca,L}$- and INa-mediated wave propagation whose relative proportions varied in time (Figure 8).

To simulate the effects of pinacidil, we added a formulation of I_{KATP}[17] whose conductance throughout the tissue increased linearly to a maximum over a specified time period. Under these conditions, the outcome of I_{KATP} activation during the arrhythmia was probabilistic in nature, sensitive to both the timing and the speed of I_{KATP} activation. When I_{KATP} was activated rapidly over 50 ms, reentry terminated and the tissue repolarized to a quiescent state in 41 of 201 trials. In the remaining 59 trials, the $I_{Ca,L}$-mediated rotor was converted to an I_{Na}-mediated rotor (Figure 8A). The specific outcome depended on whether I_{Na}-mediated wave fronts were present in the tissue when I_{KATP} was activated. If I_{KATP} was activated at a time when no I_{Na} wave fronts happened to be present in the arm of the rotor, reentry terminated (Figure 8A, unshaded areas) because no I_{Na} wave fronts were present to form a new rotor after the $I_{Ca,L}$-mediated rotor terminated. In contrast, if I_{KATP} was activated at a time when I_{Na} wave fronts were present in the arm of the rotor (Figure 8A, shaded areas), these I_{Na} wave fronts were unaffected by I_{KATP} activation. Transformation from an $I_{Ca,L}$-mediated to an I_{Na}-mediated rotor was achieved by the I_{Na}-mediated wave fronts whipping around the front end of the vanishing $I_{Ca,L}$-mediated rotor, reactivating the fully repolarized tissue previously occupied by the $I_{Ca,L}$-mediated wave front (Figure 8B).

In this scenario, the speed of I_{KATP} activation also played a critical role. When I_{KATP} was activated slowly—over 10 seconds or 5 minutes—the incidence of termination increased to

54% (101 trials) and 100% (21 trials), respectively. This is because when I_{KATP} reached a sufficient amplitude to terminate all $I_{Ca,L}$-mediated wave fronts, the AP duration and wavelength were still too long to allow an I_{Na}-mediated rotor to become sustained. That is, if an I_{Na}-mediated rotor formed at this point, it meandered to the tissue border and self-terminated (Movie 1, online supplementary material). Only if I_{KATP} continued to activate rapidly did the AP duration and wavelength shorten sufficiently to allow the I_{Na}-mediated rotor to stabilize before colliding with a tissue border and self-terminating (Movie 2, online supplementary material). If the tissue size was increased to prolong the lifetime of the I_{Na}-mediated rotor when the $I_{Ca,L}$-mediated rotor terminated, the percentage of trials that resulted in termination for the same time course of I_{KATP} activation decreased.

If random cell-to-cell variability in the number of K_{ATP} channels was introduced into the tissue model to simulate a heterogeneous distribution of K_{ATP} channels among cardiac myocytes, then for the cases in which I_{Na}-mediated rotors did not terminate during I_{KATP} activation, the increased dispersion of repolarization led to unidirectional conduction block, causing the I_{Na}-mediated rotor to break up into multiwavelet VF (Figure 8C). This was similar to the finding in monolayers in which pinacidil increased arrhythmia complexity (Figure 5B).

In summary, these simulations show that I_{KATP} activation can either terminate $I_{Ca,L}$-mediated reentry or convert it to more complex I_{Na}-mediated reentry in heterogeneous tissue, depending on the timing and speed of I_{KATP} activation, with slower I_{KATP} activation favoring termination.

Discussion

Activation of sarcolemmal K_{ATP} channels shortens the cardiac AP duration and generally suppresses EADs by increasing repolarization reserve, as demonstrated previously in many studies.[2–9] Therefore, when ventricular arrhythmias such as PVT and TdP are caused by EAD-mediated triggered activity arising from one or more focal sites, I_{KATP} activation tends to be antiarrhythmic by suppressing EAD formation. However, the extent to which EAD-mediated arrhythmias are focal or reentrant remains controversial.[20,21] We recently demonstrated that under EAD-promoting conditions, cardiac tissue can become bi-excitable, that is, capable of supporting both I_{Na}- and $I_{Ca,L}$-mediated wave fronts.[1] The theory of bi-excitability posits that myocytes can develop 2 quasi-stable resting membrane potentials under appropriate conditions in which repolarization reserve is reduced (eg, by BayK + Iso)—a fully repolarized state from which I_{Na}-mediated wave fronts emanate and a partially depolarized state at which I_{Na} is inactivated but $I_{Ca,L}$ can still mediate propagating wave fronts. We previously demonstrated this phenomenon in BayK + Iso-treated monolayers without a central obstacle in which nonsustained bursting behavior emanates from a partially depolarized membrane potential, which repolarizes back to the fully repolarized resting membrane potential when the burst terminates.[18] Here, we have shown the analogous phenomenon for $I_{Ca,L}$-mediated reentry in bi-excitable tissue. In the optical trace in Figure 2B, termination of $I_{Ca,L}$-mediated reentry by nitrendipine allowed membrane potential to fully repolarize. In Figure 4B, termination of $I_{Ca,L}$-mediated by pinacidil had a similar effect, with full repolarization and a subsequent full amplitude AP. It is possible that by

increasing repolarization reserve, pinacidil hyperpolarized the fully repolarized resting potential to some extent. However, the similarity between the effects of nitrendipine and pinacidil implies that full repolarization after pinacidil, such as nitrendipine, is primarily due to the destabilization of the partially depolarized resting state made possible by BayK + Iso, rather by additional hyperpolarization of the fully repolarized resting membrane potential by I_{KATP} activation.

$I_{Ca,L}$-mediated rotors that can form under bi-excitable conditions exhibit electrocardiographic features and cycle lengths resembling PVT and TdP.[1] Given the possibility that $I_{Ca,L}$-mediated reentry may be involved in the pathogenesis of PVT or TdP, the question arises as to whether I_{KATP} activation has exclusively antiarrhythmic effects on this form of reentry (as it does on EAD-mediated triggered activity) or whether it can be proarrhythmic as well. This is an important question, because I_{KATP} activation agonists have been proposed as therapeutic agents for TdP and also because hypotension associated with prolonged episodes of PVT and TdP may result in I_{KATP} activation physiologically. We hoped that the investigation of this issue might provide insight into why PVT and TdP episodes, which usually self-terminate, occasionally degenerate to VF to cause sudden cardiac death.[10–12]

By using pinacidil to activate I_{KATP} in NRVM monolayers, we found I_{KATP} activation often converted $I_{Ca,L}$-mediated anatomic or functional reentry to I_{Na}-mediated reentry with faster conduction velocity, accelerating the rate of the tachycardia. These findings imply that if $I_{Ca,L}$-mediated reentry is present during PVT or TdP, activation of I_{KATP} by drugs or ischemia might accelerate the tachycardia, potentially resulting in wavebreak and precipitating multiwavelet or mother rotor VF. We consistently observed that anatomic $I_{Ca,L}$-mediated reentry around a central obstacle was converted to anatomic I_{Na}-mediated reentry. For functional $I_{Ca,L}$-mediated rotors in which $I_{Ca,L}$- and I_{Na}-mediated wave fronts coexisted, however, the effects of I_{KATP} activation were probabilistic. As elucidated in computer simulations, if I_{KATP} was activated during an epoch when no I_{Na}mediated wave fronts happened to be present in the tissue, reentry terminated. However, if I_{KATP} was activated when both $I_{Ca,L}$- and I_{Na}-mediated wave fronts were present, the $I_{Ca,L}$-mediated wave fronts were eliminated but the I_{Na}-mediated wave fronts were unaffected, allowing I_{Na}-mediated rotors to form and potentially break up into multiwavelet or mother rotor VF (Figure 8). An important factor influencing whether functional $I_{Ca,L}$-mediated rotors terminated or were converted to I_{Na}-mediated reentry and VF was the rapidity with which I_{KATP} was activated. As I_{KATP} was activated more slowly, the probability of termination progressively increased and the probability of degeneration to VF concomitantly decreased. This was because the tissue size was not large enough to support a stable I_{Na}-mediated rotor when I_{KATP} first became large enough to eliminate the $I_{Ca,L}$-mediated rotor. Only if subsequent I_{KATP} activation was rapid did the AP duration and wavelength subsequently shorten quickly enough to stabilize the I_{Na}-mediated rotor before it meandered to a tissue border and self-terminated. This implies that tissue size, relative to wavelength, is also an important determinant of whether functional $I_{Ca,L}$-mediated rotors terminate or are converted to sustained I_{Na}-mediated reentry, with termination being favored by smaller tissue size. However, even for the large tissue size (4.5 cm × 4.5 cm) that we simulated, the incidence of termination was still 41% even with very rapid I_{KATP} activation over 50 ms and

100% for slow activation over 5 minutes. Given that spontaneous I_{KATP} activation due to systemic hypotension during PVT or TdP occurs gradually over minutes, our findings suggest that hypotension in this setting is more likely to favor termination of these arrhythmias than promote degeneration to VF but the latter still has a finite probability. In addition, there are many other reasons why episodes of PVT or TdP due to $I_{Ca,L}$-mediated reentry might spontaneously terminate before I_{KATP} activation becomes significant, including heterogeneity-induced spiral drifting, wave collision, and dynamical instabilities.[22–25] Also, under conditions in which PVT or TdP are maintained primarily by focal activation, rather than $I_{Ca,L}$-mediated reentry, I_{KATP} activation would be expected to suppress the arrhythmia, whether activated rapidly or slowly. However, our findings raise the possibility that an acute intravenous administration of an I_{KATP} agonist to terminate PVT or TdP in the clinical setting could run a significant risk of converting the arrhythmia to VF if the arrhythmia involved $I_{Ca,L}$-mediated reentry and the drug was administered rapidly.

In extrapolating to the clinical relevance of the present findings, a number of caveats and limitations should be recognized. $I_{Ca,L}$-mediated reentry was induced by using BayK + Iso in NRVM monolayers, which, despite the advantages for optical mapping, have important electrophysiological differences with human myocardium. It is also not possible to calibrate membrane potential absolutely by using optical mapping, although in a previous study,[19] we documented a resting membrane potential < −70 mV, as confirmed in other studies,[26,27] but values from −65 to −70 mV have also been reported,[19] at which I_{Na} may be significantly reduced. BayK + Iso is an artificial means of inducing EADs, with arguably limited direct physiological relevance, although Iso alone has been shown to generate EAD bursting in this preparation and is well known to be a potentiating arrhythmogenic factor in long QT syndromes.[28,29] Among many other effects, BayK and Iso both accentuate mode 2 gating of L-type Ca channels, which is believed to contribute to the genetic defect in LQT8.[30] In addition, $I_{Ca,L}$-mediated rotors due to bi-excitability have yet to be documented experimentally in intact native animal or human cardiac tissues subjected to more physiologically relevant stressors causing EADs. The experimental model (NRVM) and computer AP model (rabbit ventricle) also represented different species. On the other hand, the observation that different experimental and computer models yielded consistent results increases our confidence that these findings are generalizable and may have relevance to clinical EAD-mediated arrhythmias such as TdP and PVT.

Conclusions

I_{KATP} activation can have pro-arrhythmic or anti-arrhythmic effects on $I_{Ca,L}$-induced reentry in the setting of EAD-mediated arrhythmias such as TdP and PVT.

Supplementary Material

Refer to Web version on PubMed Central for supplementary material.

Acknowledgments

This study was supported by National Institutes of Health (NIH) grants P01 HL078931 (to Dr Weiss and Dr Qu), R01 HL103622 (to Dr Weiss and Dr Qu), MSTP T32GM008042, and MCIP T32GM065823; a fellowship award

for advanced researchers from the Swiss Foundation for Grants in Biology and Medicine (Dr de Lange); and the Laubisch and Kawata Endowments (to Dr Weiss).

Appendix: Supplementary data

Supplementary data associated with this article can be found in the online version at http://dx.doi.org/10.1016/j.hrthm.2012.12.017.

ABBREVIATIONS

2D	2-dimensional
AP	action potential
EAD	early afterdepolarization
$I_{Ca,L}$	L-type calcium current
I_{KATP}	ATP-sensitive K current
I_{Na}	Na current
Iso	isoproterenol
K_{ATP}	ATP-sensitive K
NRVM	neonatal rat ventricular myocyte
PVT	polymorphic ventricular tachycardia
TdP	torsades de pointes
TTX	tetrodotoxin
VF	ventricular fibrillation

References

1. Chang MG, Sato D, de Lange E, et al. Bi-stable wave propagation and early afterdepolarization-mediated cardiac arrhythmias. Heart Rhythm. 2012; 9:115–122. [PubMed: 21855520]
2. Fish FA, Prakash C, Roden DM. Suppression of repolarization-related arrhythmias in vitro and in vivo by low-dose potassium channel activators. Circ Res. 1990; 82:1362–1369.
3. Spinelli W, Sorota S, Siegal M, et al. Antiarrhythmic actions of the ATP-regulated K current activated by pinacidil. Circ Res. 1991; 68:1127–1137. [PubMed: 2009612]
4. Carlsson L, Abrahamsson C, Drews L, et al. Antiarrhythmic effects of potassium channel openers in rhythm abnormalities related to delayed repolarization. Circulation. 1992; 85:1491–1500. [PubMed: 1555289]
5. Sato T, Hata Y, Yamamoto M, Morita H, et al. Early afterdepolarization abolished by potassium channel opener in a patient with idiopathic long QT syndrome. J Cardiovasc Electrophysiol. 1995; 6:279–282. [PubMed: 7647953]
6. Riccioppo Neto F, Mesquita Junior O, Olivera GB. Antiarrhythmic and electrophysiological effects of the novel K_{ATP} channel opener, rilmakalim, in rabbit cardiac cells. Gen Pharmacol. 1997; 29:201–205. [PubMed: 9251899]
7. Watanabe O, Okumura T, Takeda H, et al. Nicorandil, a potassium channel opener, abolished torsades de pointes in a patient with complete atrioventricular block. Pacing Clin Electrophysiol. 1999; 22:686–688. [PubMed: 10234727]

8. Shimizu W, Antzelevitch C. Effects of a K channel opener to reduce transmural dispersion of repolarization and prevent torsade de pointes in LQT1, LQT2, and LQT3 models of the long-QT syndrome. Circulation. 2000; 102:706–712. [PubMed: 10931813]
9. Chinushi M, Kasai H, Tagawa M, et al. Triggers of ventricular tachyarrhythmias and therapeutic effects of nicorandil in canine models of LQT2 and LQT3 syndromes. J Am Coll Cardiol. 2002; 40:555–562. [PubMed: 12142125]
10. Krikler DM, Curry PV. Torsade de pointes, an atypical ventricular tachycardia. Br Heart J. 1976; 38:117–120. [PubMed: 1259825]
11. El-Sherif N, Turitto G. Torsade de pointes. Curr Opin Cardiol. 2003; 18:6–13. [PubMed: 12496496]
12. Drew BJ, Ackerman MJ, Funk M, et al. Prevention of torsade de pointes in hospital settings: a scientific statement from the American Heart association and the American College of Cardiology Foundation. Circulation. 2010; 121:1047–1060. [PubMed: 20142454]
13. Abraham MR, Henrikson CA, Tung L, et al. Antiarrhythmic engineering of skeletal myoblasts for cardiac transplantation. Circ Res. 2005; 97:159–167. [PubMed: 15976318]
14. de Diego C, Pai RK, Dave AS, et al. Spatially discordant alternans in cardiomyocyte monolayers. Am J Physiol Heart Circ Physiol. 2008; 294:H1417–H1425. [PubMed: 18223190]
15. Calmettes G, Drummond GB, Vowler SL. Making do with what we have: use your bootstraps. J Physiol. 2012; 590:3403–3406. [PubMed: 22855048]
16. Mahajan A, Shiferaw Y, Sato D, et al. A rabbit ventricular action potential model replicating cardiac dynamics at rapid heart rates. Biophys J. 2008; 94:392–410. [PubMed: 18160660]
17. Ferrero JM Jr, Saiz J, Ferrero JM, et al. Simulation of action potentials from metabolically impaired cardiac myocytes: role of ATP-sensitive K current. Circ Res. 1996; 79:208–221. [PubMed: 8755997]
18. Chang MG, Chang CY, de Lange E, et al. Dynamics of early afterdepolarization-mediated triggered activity in cardiac monolayers. Biophys J. 2012; 102:2706–2714. [PubMed: 22735520]
19. Chang MG, Zhang Y, Chang CY, et al. Spiral waves and reentry dynamics in an in vitro model of the healed infarct border zone. Circ Res. 2009; 105:1062–1071. [PubMed: 19815825]
20. Asano Y, Davidenko JM, Baxter WT, et al. Optical mapping of drug-induced polymorphic arrhythmias and torsade de pointes in the isolated rabbit heart. J Am Coll Cardiol. 1997; 29:831–842. [PubMed: 9091531]
21. Choi BR, Burton F, Salama G. Cytosolic Ca triggers early afterdepolarizations and torsade de pointes in rabbit hearts with type 2 long QT syndrome. J Physiol. 2002; 543:615–631. [PubMed: 12205194]
22. Nattel S, Kneller J, Zou R, et al. Mechanisms of termination of atrial fibrillation by class I antiarrhythmic drugs: Evidence from clinical, experimental, and mathematical modeling studies. J Cardiovasc Electrophysiol. 2003; 14:S133–S139. [PubMed: 14760915]
23. Qu Z, Weiss JN. Effects of Na and K channel blockade on vulnerability to and termination of fibrillation in simulated normal cardiac tissue. Am J Physiol Heart Circ Physiol. 2005; 289:H1692–H1701. [PubMed: 15937096]
24. Qu Z. Critical mass hypothesis revisited: Role of dynamical wave stability in spontaneous termination of cardiac fibrillation. Am J Physiol. 2006; 290:H255–H263.
25. Yamazaki M, Honjo H, Nakagawa H, et al. Mechanisms of destabilization and early termination of spiral wave reentry in the ventricle by a class III antiarrhythmic agent, nifekalant. Am J Physiol Heart Circ Physiol. 2007; 292:H539–H548. [PubMed: 16936005]
26. Sekar RB, Kizana E, Cho HC, et al. IK1 heterogeneity affects genesis and stability of spiral waves in cardiac myocyte monolayers. Circ Res. 2009; 104:355–364. [PubMed: 19122180]
27. Pedrotty DM, Klinger RY, Kirkton RD, et al. Cardiac fibroblast paracrine factors alter impulse conduction and ion channel expression of neonatal rat cardiomyocytes. Cardiovasc Res. 2009; 83:688–697. [PubMed: 19477968]
28. Kossmann CE. The long QT interval and syndromes. Adv Intern Med. 1987; 32:87–110. [PubMed: 3548260]
29. Vermeulen JT. Mechanisms of arrhythmias in heart failure. J Cardiovasc Electrophysiol. 1998; 9:208–221. [PubMed: 9511895]

30. Splawski I, Timothy KW, Decher N, et al. Inaugural article: Severe arrhythmia disorder caused by cardiac L-type calcium channel mutations. Proc Natl Acad Sci. 2005; 102:8089–8096. [PubMed: 15863612]

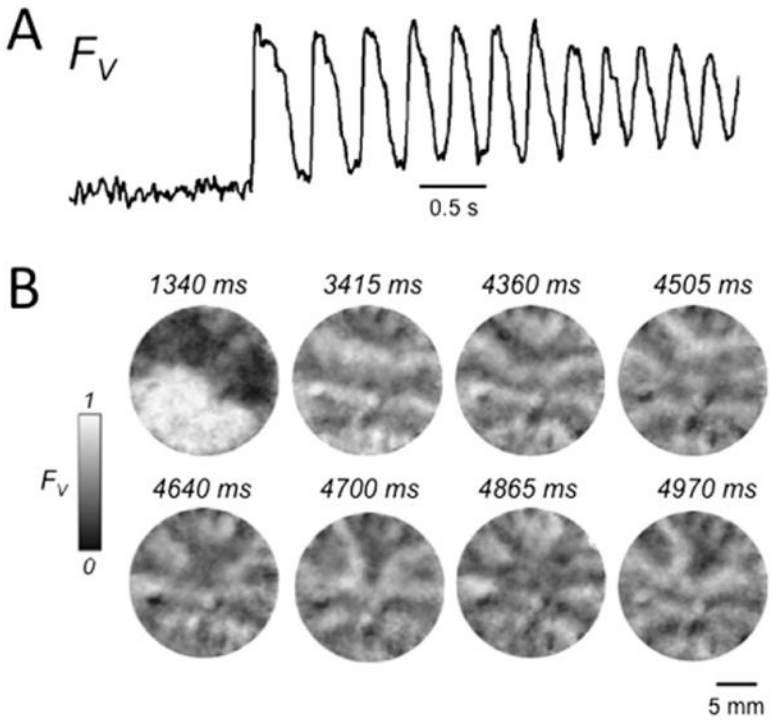

Figure 1.

Early afterdepolarization (EAD)-related arrhythmias induced by BayK4688 + isoproterenol in neonatal rat ventricular myocyte monolayers. **A:** Optical voltage trace (F_V) illustrating a burst of EAD-mediated triggered activity following a paced beat. Note the incomplete repolarization between beats. **B:** Snapshots of voltage fluorescence (F_V) at the times indicated following the paced beat at 1340 ms, revealing a complex pattern of wave fronts due to a mixture of focal activity and reentry. F_V is shown on a gray scale, with 0 = maximally repolarized (<−70 mV) and 1 = maximally depolarized (>0 mV), on the basis of our previously reported patch electrode recording estimates.[19]

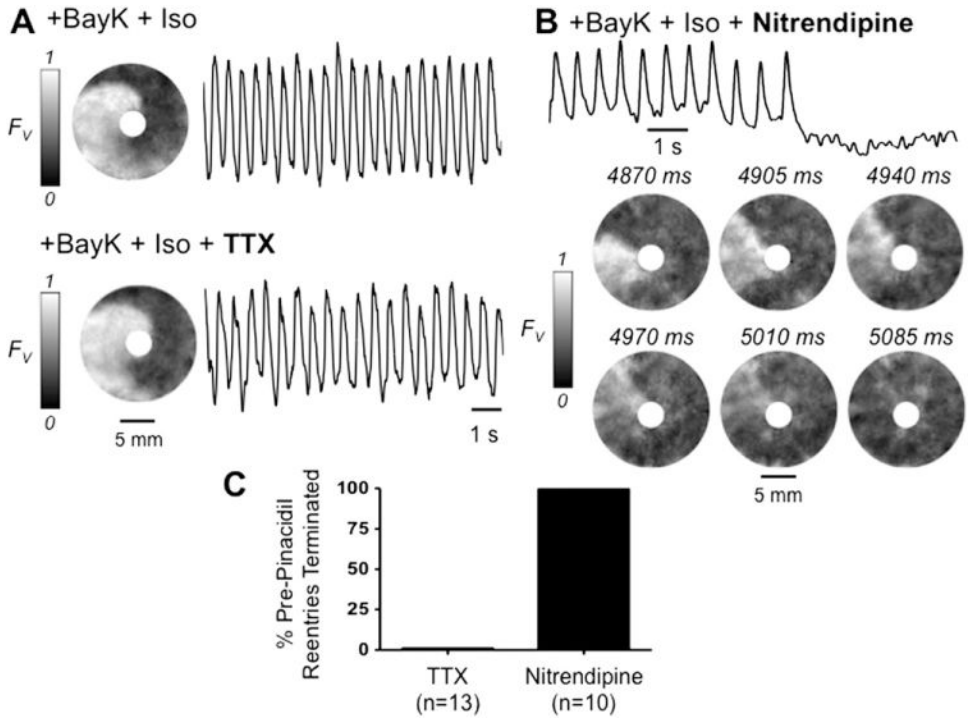

Figure 2.

Early afterdepolarization-related reentry around a central obstacle in a neonatal rat ventricular myocyte monolayer. **A:** Snapshot (left) and trace (right) of voltage fluorescence (F_V), illustrating that reentry around the central obstacle was unaffected by tetrodotoxin (TTX) (50 μM). **B:** In contrast, nitrendipine (5 μM) terminated reentry. **C:** Bar graph summarizing incidence of termination of reentry by tetrodotoxin (TTX) vs nitrendipine in 23 monolayers. F_V gray scale as described in Figure 1 legend. BayK + Iso = BayK4688 + isoproterenol.

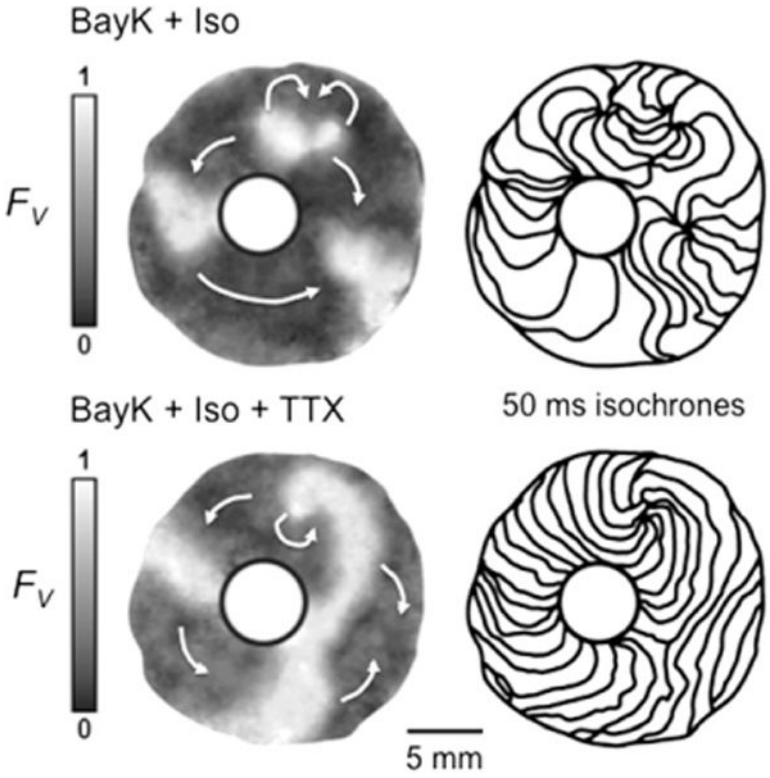

Figure 3.

Effect of tetrodotoxin (TTX) on early afterdepolarization (EAD)-related reentry around a central obstacle in a neonatal rat ventricular myocyte monolayer. Top panels: Sustained reentry was driven by a figure-eight rotor (curved arrows at 1 o'clock). At right, isochrone maps (50 ms between isochrones) show slow propagation (closely spaced isochrones) clockwise from 9 to 6 o'clock, consistent with L-type calcium current ($I_{Ca,L}$)-mediated propagation, but much faster (widely spaced isochrones) from 6 to 9 o'clock, consistent with a significant contribution of Na current (INa)-mediated propagation. Bottom panels: After TTX (50 μM), a single rotor with the same cycle length (~500 ms) continues, but conduction velocity is now uniformly slow, consistent with $I_{Ca,L}$-mediated rotor and wave propagation throughout the tissue. F_V gray scale as described in Figure 1 legend. BayK + Iso = BayK4688 + isoproterenol.

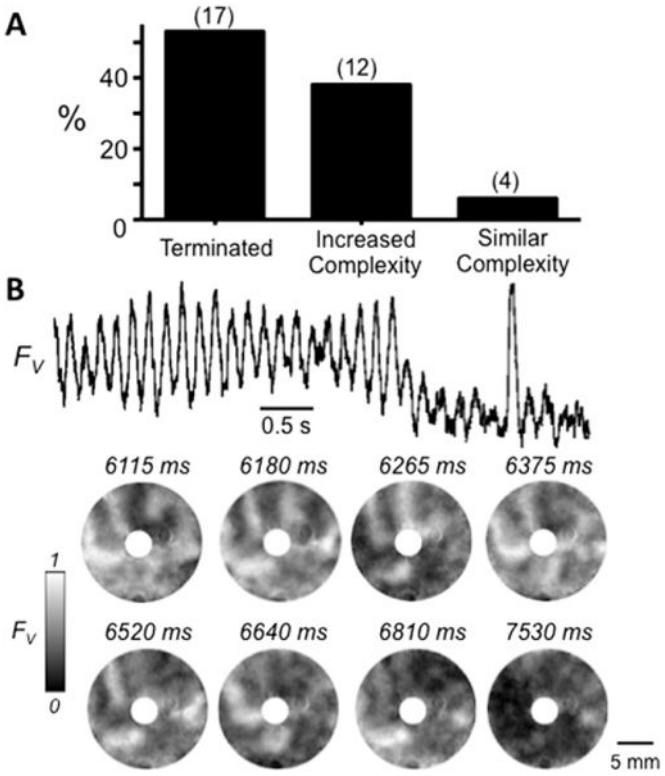

Figure 4.

Effect of the ATP-sensitive K channel agonist pinacidil in neonatal rat ventricular myocyte (NRVM) monolayers with complex sustained early afterdepolarization (EAD)-mediated arrhythmias. **A**: Histogram illustrating the outcomes of pinacidil (100 μM) treatment on complex EAD-mediated arrhythmias induced by BayK4688 + isoproterenol in 33 NRVM monolayers with a central obstacle. **B**: Representative optical trace (top) and snapshots (below) of voltage fluorescence (F_V) at the times indicated, illustrating termination of a complex EAD-mediated arrhythmia by pinacidil. In this example, the arrhythmia was driven primarily by a functional rotor (spiral wave) at 1 o'clock. F_V gray scale as described in Figure 1 legend.

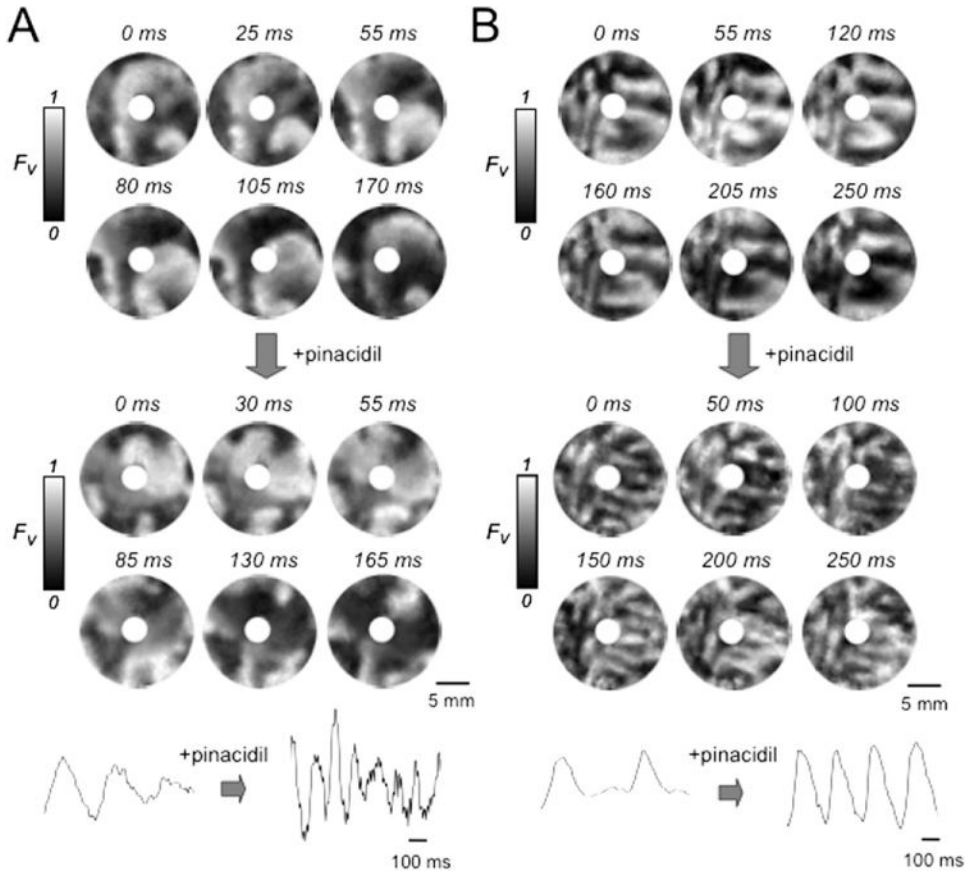

Figure 5.

Effect of the ATP-sensitive K channel agonist pinacidil in neonatal rat ventricular myocyte monolayers with complex sustained early afterdepolarization-mediated arrhythmias. **A:** Snapshots of voltage fluorescence (F_V) at the times indicated in a monolayer with a central obstacle in which BayK4688 + isoproterenol induced an arrhythmia driven primarily by functional rotors (spiral waves) at 6 and 8 o'clock (left panels). Pinacidil (100 μM, right panels) accelerated but did not significantly affect the complexity of the arrhythmia. **B:** Voltage snapshots from another monolayer with a central obstacle, in which pinacidil (right panels) increased the complexity of the BayK4688 + isoproterenol-induced arrhythmia, as evident from the greater number of wave fronts. F_V gray scale as described in Figure 1 legend.

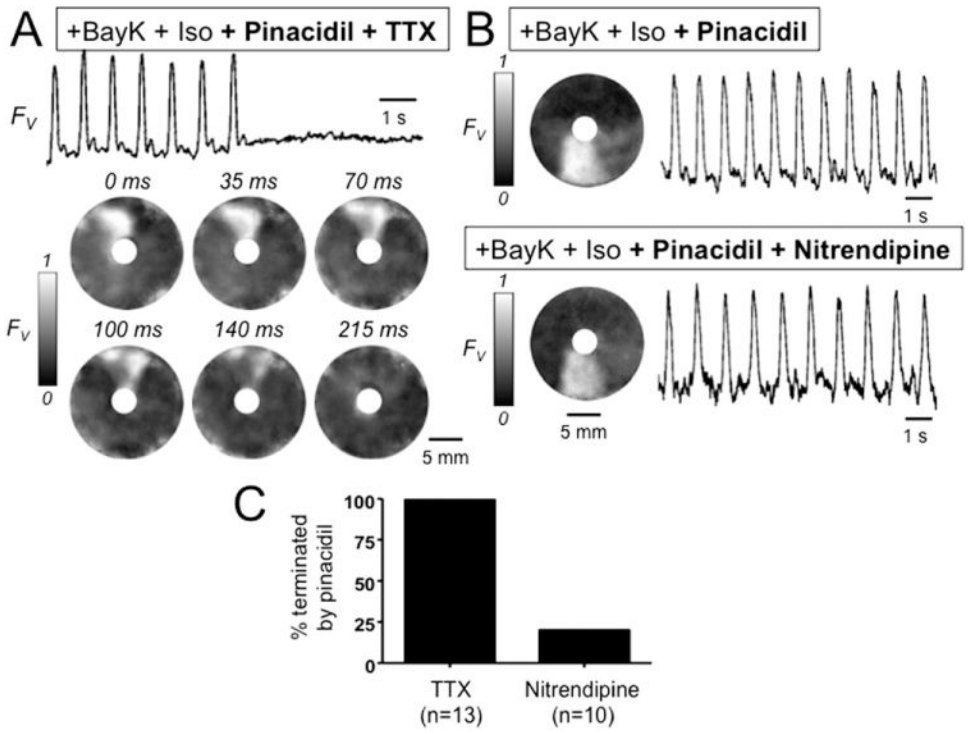

Figure 6.

Effect of pinacidil on early afterdepolarization-mediated reentry around a central obstacle in a neonatal rat ventricular myocyte monolayer. **A:** Optical trace (above) and snapshots (below) of voltage fluorescence (F_V) in a monolayer in which BayK4688 + isoproterenol induced sustained reentry around a central obstacle. After pinacidil treatment, the addition of tetrodotoxin (TTX) (50 μM) terminated reentry. **B:** Same, but with nitrendipine (5 μM) added instead of TTX, showing that reentry persists. **C:** Bar graph summarizing the incidence of termination of reentry by TTX vs nitrendipine in 23 monolayers exposed to BayK4688 + isoproterenol + pinacidil. F_V gray scale as described in Figure 1 legend. BayK + Iso = BayK4688 + isoproterenol.

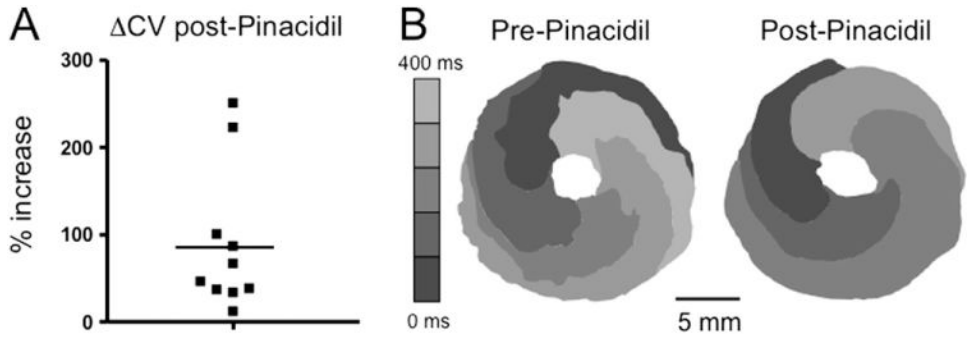

Figure 7.

Effect of pinacidil on conduction velocity of early afterdepolarization-mediated reentry around a central obstacle in neonatal rat ventricular myocyte monolayers. **A:** The percent increase in conduction velocity after pinacidil in 10 monolayers (solid squares) in which BayK4688 + isoproterenol induced sustained reentry around a central obstacle. Mean increase is indicated by the horizontal bar. **B:** Isochrome map during reentry in a representative monolayer, pre-, and post-pinacidil treatment. Increased spacing between 80-ms isochrome lines after pinacidil reflects increased conduction velocity. F_V gray scale as described in Figure 1 legend.

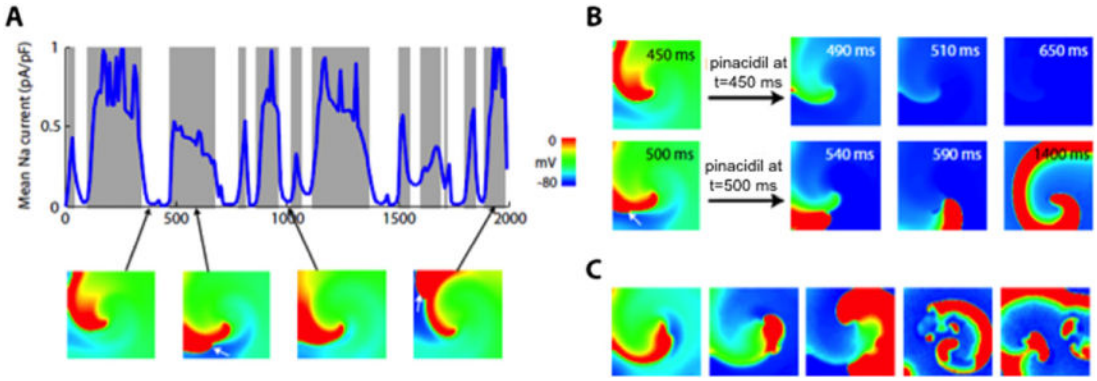

Figure 8.

Effect of ATP-sensitive K current (I_{KATP}) activation on L-type calcium current ($I_{Ca,L}$)-mediated reentry in simulated 2-dimensional heterogeneous cardiac tissue (300 × 300 myocytes). **A:** Outcomes of rapidly activating I_{KATP} at various time points during reentry driven by an $I_{Ca,L}$-mediated rotor in the center of the tissue. Gray zones indicate that $I_{Ca,L}$-mediated reentry converted to Na current (I_{Na})-mediated reentry after I_{KATP} activation; white zones indicate that reentry terminated. The blue line shows I_{Na} amplitude averaged over all cells in the tissue over time. I_{KATP} activation terminated reentry only if no significant I_{Na}-mediated wave fronts were present. Voltage snapshots (below) show the $I_{Ca,L}$-mediated rotor in the center of the tissue, with I_{Na}-mediated wave fronts intermittently present along the spiral arm (2nd and 4th panels; white arrows). **B:** Voltage snapshots showing termination of reentry by I_{KATP} activation at t = 450 ms (top row) but conversion to I_{Na}-mediated reentry at t = 500 ms (bottom row). **C:** When the number of K_{ATP} channels was randomly varied from myocyte to myocyte (using a Gaussian distribution with mean 3.8 channels/μm2 and standard deviation 2.0), I_{KATP} activation caused the stable $I_{Ca,L}$-mediated rotor to convert to an I_{Na}-mediated rotor, which then broke up into multiwavelet VF. F_V scale as described in Figure 1 legend.